Cell

Drosophila Auditory Organ Genes and Genetic Hearing Defects

Pingkalai R. Senthilan,[1,4,5] David Piepenbrock,[1,4] Guvanch Ovezmyradov,[1] Björn Nadrowski,[1,6] Susanne Bechstedt,[2,7] Stephanie Pauls,[1] Margret Winkler,[1] Wiebke Möbius,[3] Jonathon Howard,[2] and Martin C. Göpfert[1,*]
[1]Department of Cellular Neurobiology, University of Göttingen, Julia-Lermontowa-Weg 3, 37077 Göttingen, Germany
[2]Max-Planck-Institute for Cell Biology and Genetics, Pfotenhauerstrasse 108, 01307 Dresden, Germany
[3]Max-Planck-Institute for Experimental Medicine, Hermann-Rein-Strasse 5, 37075 Göttingen, Germany
[4]These authors contributed equally to this work
[5]Present address: Neurobiology & Genetics, University of Würzburg, Am Hubland, 97074 Würzburg, Germany
[6]Present address: Department of Theoretical Physics, University of Saarland, Campus E2 6, 66123 Saarbrücken, Germany
[7]Present address: Department of Biology, McGill University, 1205 Avenue Docteur Penfield, Montréal, Québec H3A 1B1, Canada
*Correspondence: mgoepfe@gwdg.de
http://dx.doi.org/10.1016/j.cell.2012.06.043

SUMMARY

The *Drosophila* auditory organ shares equivalent transduction mechanisms with vertebrate hair cells, and both are specified by *atonal* family genes. Using a whole-organ knockout strategy based on *atonal*, we have identified 274 *Drosophila* auditory organ genes. Only four of these genes had previously been associated with fly hearing, yet one in five of the genes that we identified has a human cognate that is implicated in hearing disorders. Mutant analysis of 42 genes shows that more than half of them contribute to auditory organ function, with phenotypes including hearing loss, auditory hypersusceptibility, and ringing ears. We not only discover ion channels and motors important for hearing, but also show that auditory stimulus processing involves chemoreceptor proteins as well as phototransducer components. Our findings demonstrate mechanosensory roles for ionotropic receptors and visual rhodopsins and indicate that different sensory modalities utilize common signaling cascades.

INTRODUCTION

Hearing impairment is the most common sensory deficit in humans (Hildebrand et al., 2008). Various forms of hearing impairment have genetic causes, but many of the responsible genes continue to remain elusive (Petit, 2006; Dror and Avraham, 2009). One of the genetic model organisms that is used to search for auditory relevant genes is *Drosophila*, which communicates via courtship songs and hears with antennal ears (Lu et al., 2009).

The ear of *Drosophila* consists of a sound receiver and an auditory sensory organ. The sound receiver is formed by the third antennal segment and its feathery arista (Göpfert and Robert, 2001) (Figure 1A). Vibrations of this antennal receiver are transduced by Johnston's organ (JO), an array of ~250 chordotonal sensilla in the antenna's second segment that serve hearing as well as wind and gravity sensing (Kamikouchi et al., 2009; Yorozu et al., 2009). JO sensilla are composed of mechanosensory neurons and supporting cells that are derived from sensory organ precursors by lineage (Eberl and Boekhoff-Falk, 2007). These precursors and the identity of the lineage are specified by the basic helix-loop-helix (bHLH) transcription factor Atonal (Ato) (Jarman et al., 1993), whose homolog AtoH1 (also known as Math1) directs the formation of hair cells in vertebrate ears (Bermingham et al., 1999).

Apart from Ato, JO sensilla and hair cells also share other proteins, including myosin VIIa (Weil et al., 1995; Todi et al., 2005), certain transient receptor potential (TRP) channels (Liedtke et al., 2000; Walker et al., 2000; Sidi et al., 2003; Kim et al., 2003), and prestins (Zheng et al., 2000; Weber et al., 2003). JO neurons and hair cells also function in similar manners, though the neurons use primary cilia instead of actin-based hair bundles as sensory organelles: both cell types employ physically equivalent transduction modules that seem to consist of force-gated ion channels, adaptation motors, and gating springs (Albert et al., 2007; Gillespie and Müller, 2009). Both cell types also use these modules to actively amplify their mechanical input, explaining why the *Drosophila* ear displays all the hallmarks of active mechanical amplification known from vertebrate ears (Hudspeth, 2008; Nadrowski et al., 2008).

Notwithstanding the fly's amenability to genetic dissection, rather few auditory relevant *Drosophila* genes have been described and key molecules such as the auditory transduction channels still await their molecular identification in vertebrates and flies (Gillespie and Müller, 2009; Lu et al., 2009): According to the Gene Ontology (GO) database (Ashburner et al., 2000), 24 annotated *Drosophila* genes are associated with the "sensory perception of sound" (GO: 0007605; Table S1 available online), which compares to some 130 genes this GO term currently includes for mice. The 24 auditory relevant fly genes have mostly emerged from forward genetics screens (Kernan et al., 1994; Eberl et al., 1997, 2000), yet linking mutations to genes is time consuming and several mutations that affect fly hearing remain uncharacterized. An attractive alternative to forward genetics is reverse genetics, in which candidate genes are narrowed down by expression profiling prior to testing for mutant

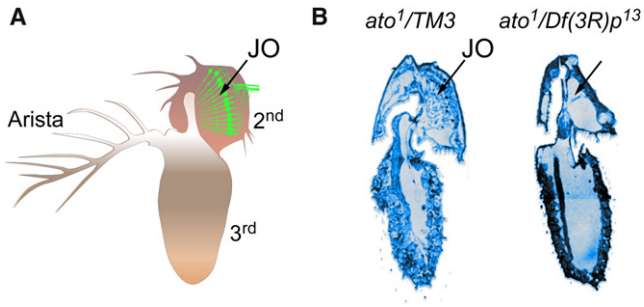

Figure 1. Antennal Ear of *Drosophila*

(A) Sketch of the fly's antenna depicting its second and third segments and the arista. The second segment harbors JO (green).

(B) Longitudinal antennal sections from *ato*^{1}/*TM3* controls and *ato*^{1}/*Df(3R)p*^{13} mutants. In the mutants, JO is lost.

For a compilation of auditory relevant *Drosophila* genes, please see Table S1.

phenotypes. This approach has identified genes of, e.g., Merkel cells (Haeberle et al., 2004), hair cells (McDermott et al., 2007), campaniform mechanoreceptors (Bechstedt et al., 2010), and developing chordotonal organs (Cachero et al., 2011), and is used here to identify genes that are expressed in—and required for the auditory function of—JO. The approach we use, however, is different: instead of comparing gene expression across different cells or tissues (e.g., Haeberle et al., 2004; McDermott et al., 2007; Bechstedt et al., 2010, Cachero et al., 2011), we employ an *ato*-based knockout strategy and compare the gene expression profiles of second antennal segments with and without JO.

RESULTS

ato-Based Screening Strategy Identifies Auditory Organ Genes

Hemizygous *ato*^{1}/*Df(3R)p*^{13} null mutants lack JO in their second antennal segments (Jarman et al., 1995) (Figure 1B). Profiting from this genetic organ ablation, we screened for genes that are expressed in JO by comparing the second antennal segment transcriptomes between *ato*^{1}/*Df(3R)p*^{13} mutants and balanced *Df(3R)p*^{13}/*TM3* and *ato*^{1}/*TM3* controls (Figure 2A). To assess transcriptomes, we isolated the second antennal segments of ~50 flies per strain and extracted their total RNA. Because about half of the JO cells are sensory neurons, we also isolated RNA from the brains of *ato*^{1}/*TM3* controls to delineate neuronal genes. cRNA was hybridized to DNA microarrays containing fourteen 25 mer oligonucleotides from 18,769 probe sets for different *Drosophila* transcripts. For each experiment, three biological replicates were run (Figure 2A).

To evaluate the quality of the microarray results, several tests were performed. First, we subjected the expression profiles to cluster analysis. We found that all the three replicates of each microarray experiment cluster together, and that replicates from different experiments are distinct (Figure 2B). Second, we selected 15 transcripts covering the entire intensity range covered by the microarray data using a random stratified sampling strategy and quantified their expression in the second antennal segment with quantitative real-time polymerase chain reaction (qRT-PCR). Fold changes in expression correlated with those obtained with the microarrays (Figure 2C), globally validating the microarray results (Miron et al., 2006). Third, scatter plots (Figure 2D) documented highly correlated expression profiles for the two control strains and revealed that certain transcripts are downregulated in the second antennal segments of *ato*^{1} nulls. We assessed this differential expression with two-sample t tests using a false discovery rate procedure to correct for the multiplicity of testing. Only differential expression with a false discovery rate < 0.1 was considered significant, and only genes that were significantly enriched in the second antennal segments of both *Df(3R)p*^{13}/*TM3* and *ato*^{1}/*TM3* controls were taken into consideration (Figure 2E). We thus obtained a consensus list of 282 transcripts representing 274 genes that are downregulated if JO is absent and thus deemed to be expressed in JO. One hundred one of these JO genes display higher expression levels in JO than in the brain and 173 genes seem to be neuronal genes that are equally or more abundant in the brain (Tables S2 and S3).

The Auditory Organ Gene Set

To annotate the list of JO genes, we tested for enriched Gene Ontology terms using the AMIGO enrichment tool (Carbon et al., 2009). We found that 201 of the 274 genes are described by Gene Ontology terms, and that significant proportions of these genes encode ion channels (GO:0005216, 18 of 189 genes in this category, $p = 1.5e^{-6}$) and motors (GO:0003774, 9 of 82 genes, $p = 9.0e^{-3}$) and are implicated in the response to abiotic stimuli (GO:0009628, 36 of 198 genes, $p = 2.1e^{-21}$) and light (GO:0009416, 26 of 110 genes, $p = 1.3e^{-20}$) (Figure 3).

Motors that were identified are the myosin III NINAC, the kinesin Klp68D, and several axonemal dyneins. Ion channels include members of the ionotropic receptor (IR) family of chemoreceptors (Benton et al., 2009) and five TRPs. Two of these TRPs (Nan, Iav) are reportedly expressed in the sensory cilia of JO neurons and required for hearing (Kim et al., 2003; Gong et al., 2004). The remaining TRPs serve hygrosensation (WTRW) (Liu et al., 2007) as well as phototransduction and thermosensation (TRP, TRPL) (Montell et al., 1985; Hardie and Minke, 1992; Niemeyer et al., 1996; Rosenzweig et al., 2008). Apart from TRP and TRPL, we identified many other key components of the fly's phototransduction cascade, including the visual arrestin Arr2 (Yamada et al., 1990), the G protein subunits Gβ76C (Yarfitz et al., 1991) and Gγ30A (Schulz et al., 1999), phospholipase C (encoded by *norpA;* Bloomquist et al., 1988), protein kinase C (encoded by *inaC*; Schaeffer et al., 1989), the scaffolding protein INAD (Shieh and Niemeyer, 1995), and four of the fly's seven rhodopsins (Rhs) (Figure 3).

The list is also enriched for genes included in the *Drosophila* cilium and basal body database (Laurençon et al., 2007) (30 of 815 genes, $p = 4.8e^{-6}$) and for genes that are enriched in mechanoreceptors of the *Drosophila* haltere (Bechstedt et al., 2010) (62 of 621 genes, $p = 8.8e^{-29}$) (Figure 3). The list further comprises 12 of 100 putative chordotonal organ genes ($p = 2.4e^{-7}$) that, 3 hr after the onset of neural development, are upregulated in *ato*-expressing cells of *Drosophila* larvae (Cachero et al., 2011). Of the fly genes that are associated with

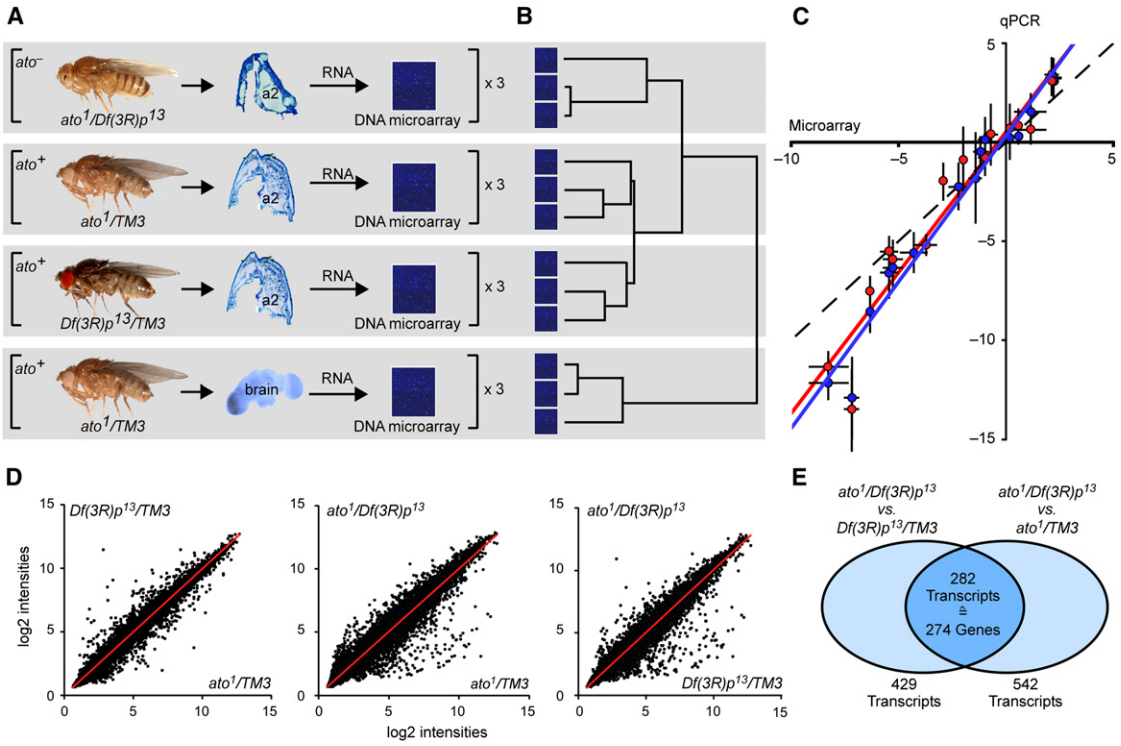

Figure 2. Identifying Auditory Organ Genes

(A) Strategy for gene identification. RNA was extracted from the second antennal segments (a2) of *ato*^{1}/*Df(3R)p*^{13} mutants and *ato*^{1}/*TM3* and *Df(3R)p*^{13}/*TM3* controls and subjected to microarray analysis. Brains of *ato*^{1}/*TM3* controls served as a neuronal control tissue. For each experiment, three biological replicates were run.

(B) Cluster analysis of the microarray data. The panel is aligned with the scheme in (A).

(C) Comparison of microarray and qRT-PCR data. Points: log2 fold changes in the expression of 15 selected genes in the second antennal segment of *ato*^{1}/*Df(3R)p*^{13} mutants with respect to those of *ato*^{1}/*TM3* (red) and *Df(3R)p*^{13}/*TM3* (blue) controls (data are presented as mean ± 1 SD, $N_{microarray}$ = 3, N_{qPCR} = 9). Continuous lines: respective linear regressions (least square). Red line: *ato*^{1}/*Df(3R)p*^{13} mutants *vs.* *ato*^{1}/*TM3* controls, slope = 1.42, Y-intercept = 0.63, R^2 = 0.92, concordance correlation coefficient (ccc) = 0.89. Blue line: *ato*^{1}/*Df(3R)p*^{13} mutants *vs.* *Df(3R)p*^{13}/*TM3* controls, slope = 1.48, Y-intercept = 0.43, R^2 = 0.96, ccc = 0.89. Hatched line: Y = X.

(D) Scatter plots of the microarray data. Each point represents the mean log2 intensity of one transcript (N = 18,769 transcripts, n = 3 replicates). Red lines: linear regressions (least square). Left: *Df(3R)p*^{13}/*TM3* controls *vs.* *ato*^{1}/*TM3* controls (regression: slope = 1.0, Y-intercept = 0.0, R^2 = 0.98; ccc = 0.99); middle: *ato*^{1}/*Df(3R)p*^{13} mutants *vs.* *ato*^{1}/*TM3* controls (regression: slope = 1.0, Y-intercept = 0.09, R^2 = 0.95; ccc = 0.97); right: *ato*^{1}/*Df(3R)p*^{13} mutants *vs.* *Df(3R)p*^{13}/*TM3* controls (regression: slope = 1.0, Y-intercept = 0.02, R^2 = 0.96; ccc = 0.98).

(E) Venn diagram depicting the number of transcripts whose expression is significantly reduced in the second antennal segments of *ato*^{1}/*Df(3R)p*^{13} mutants when compared to *Df(3R)p*^{13}/*TM3* and *ato*^{1}/*TM3* controls. The 282 transcripts in the intersection include dual hits for eight genes (*Ank2*, *CG17378*, *CG8086*, *dlg1*, *Gγ30A*, *MESK2*, *norpA*, *Sh*).

For the corresponding microarray data, please see Table S2.

hearing (Table S1), we identified *tilB* (Kavlie et al., 2010) and *eys* (Cook et al., 2008) along with *iav* and *nan*. Auditory relevant genes that are missing such as *ato*, *btv*, *ck*, *nompB*, and *ct* (Table S1) are mostly implicated in JO formation and may not be transcribed in adults. Also *nompC*, which encodes the fly's TRPN1 channel, was not detected, presumably because the respective microarray probe was directed against the 3′ end of only one isoform (isoform A; Walker et al., 2000), beyond the stop codon. A gene that was identified is *yuri*, which is expressed in a subpopulation of JO neurons and implicated in gravity sensing (Baker et al., 2007). The list also comprises at least 13 of the 1,037 zebrafish hair cell genes defined by McDermott et al. (2007) (Figure 3) and, according to the Homophila database (Chien et al., 2002), every fifth JO gene that we identified has a human cognate that is implicated in hearing disorders (Table S4).

Gene Expression in the Auditory Organ

To validate the list of JO genes, we selected 14 genes representing diverse families and analyzed their expression in the second antennal segment by in situ hybridization (Figures 4A and 4B). Genes that were chosen are four phototransduction genes (*Arr2*, *Gβ76C*, *Rh3*, and *Rh6*), two TRPs (*trpl* and *wtrw*), one IR (*Ir75d*), one axonemal dynein (*Dhc93AB*), *Bmcp*, which encodes a solute carrier (SLC) family member, *Os-C*, which encodes a putative pheromone-binding protein (McKenna et al., 1994), and the homologs of human *outer dense fiber of sperm tails 3-like 2* (*ODF3L2*) *CG8086*, human *heat shock protein beta-1*

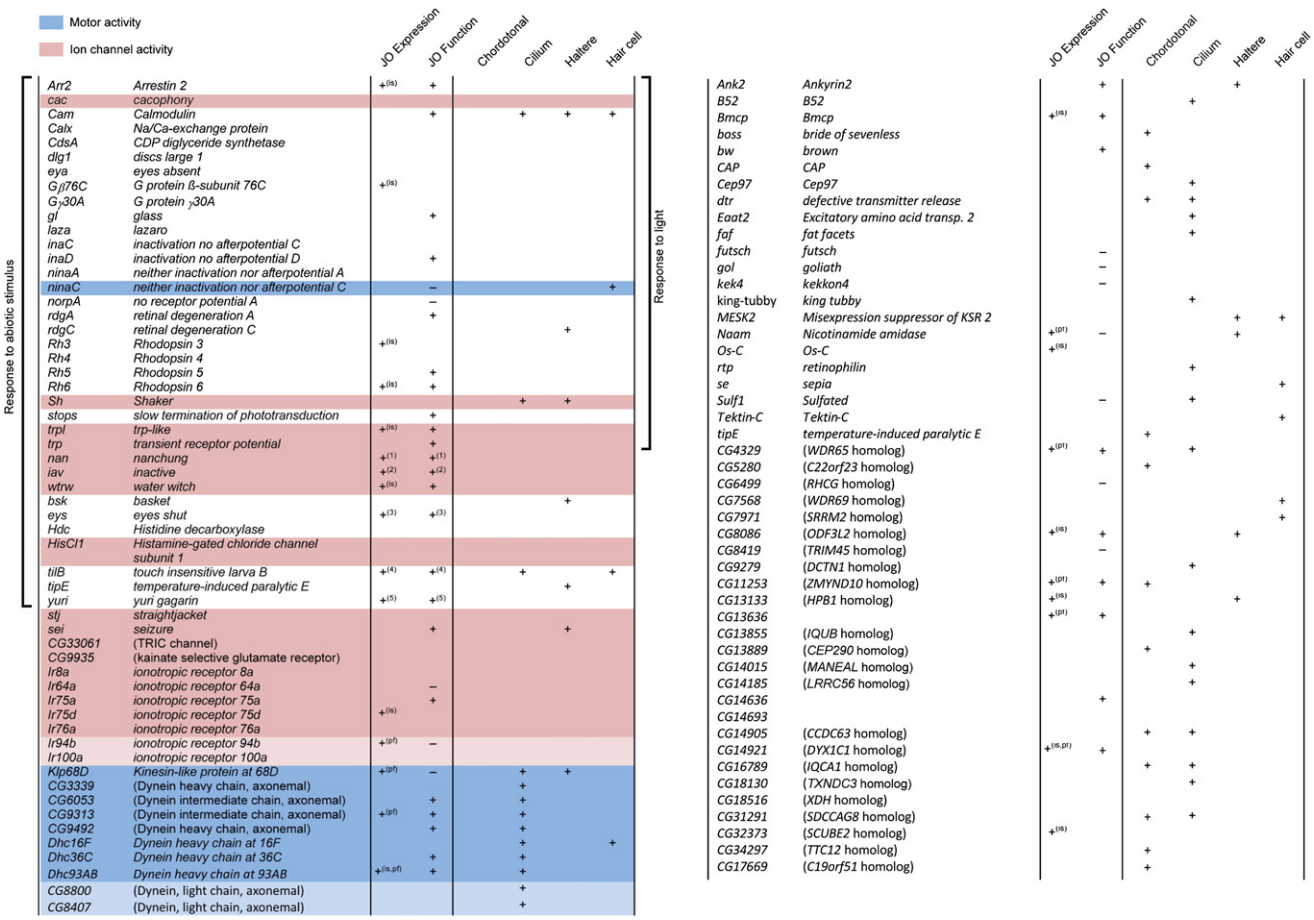

Figure 3. Auditory Organ Genes

Selection of JO genes, representing significantly enriched Gene Ontology categories and as well as chordotonal organ, cilium, hair cell, and *Drosophila* haltere genes defined by Cachero et al. (2011), Laurençon et al. (2007), McDermott et al. (2007), and Bechstedt et al. (2010), respectively. Light colors indicate channels and motors whose gene ontology annotation is pending. In the column "JO expression," + indicates that expression in JO was observed earlier or is supported by in situ hybridization [(is)] or promoter-fusion constructs [(pf)] (Figure 4). In the column "JO function," + indicates that mutations were found to alter JO function, and – indicates that no such alterations were detected (Figures 5 and 6). [(1)]Kim et al. (2003); [(2)]Gong et al. (2004); [(3)]Cook et al. (2008); [(4)]Kavlie et al. (2010); [(5)]Baker et al. (2007).

For the entire gene list and respective homologs, see Table S3. For human cognate genes that are implicated in hearing disorders, please see Table S4.

(*HSPB1*) *CG13133*, human *dyslexia susceptibility 1 candidate 1* (*DYX1C1*) *CG14921*, and human *signal peptide*, *CUB domain*, *EGF-like 2* (*SCUBE2*) *CG32373* (Table S3). Hybridization to RNA in antennal sections revealed that all the 14 genes are expressed in JO, whereas corresponding sense strand controls gave no hybridization signals (Figure 4B).

To also gain insights into cellular expression patterns, we again selected nine genes and generated transgenic flies expressing Gal4 promoter fusion constructs (Figures 4C and 4D). Individual lines were crossed to UAS-2xEGFP reporters and tested for expression in their second antennal segments. Genes that were chosen are again *Dhc93AB* and the *DYX1C1* homolog *CG14921* as well as the IR *Ir94b*, the kinesin *Klp68D*, the axonemal dynein *CG9313*, the nicotinamide amidase *Naam*, the homolog of human *WD-repeat domain 65* (*WDR65*) *CG4329*, the homolog of human *zinc finger MYND-type containing 10* (*ZMYND10*) *CG11253*, and *CG13636* whose molecular and biological functions are unknown.

All nine transgenes labeled specific cells of JO (Figure 4B): *Ir94b-Gal4*-labeled JO ligament cells that envelope the neurons' somata and anchor them in the second antennal segment. *Naam-Gal4*-labeled JO scolopale cells that wrap the cilia of the neurons and form an endolymph space. The remaining transgenes labeled some (*CG14921-Gal4*, *CG11253-Gal4*, *CG13636-Gal4*) or virtually all (*Dhc93AB-Gal4*, *CG9313-Gal4*, *CG4329-Gal4*) JO neurons. All the genes that we selected thus are expressed in JO.

Gene Requirements for Auditory Organ Function

To determine whether the list includes new genes for hearing, we selected 42 genes and tested for mutant alterations in JO function (Figures 5 and 6). Genes were chosen based on the

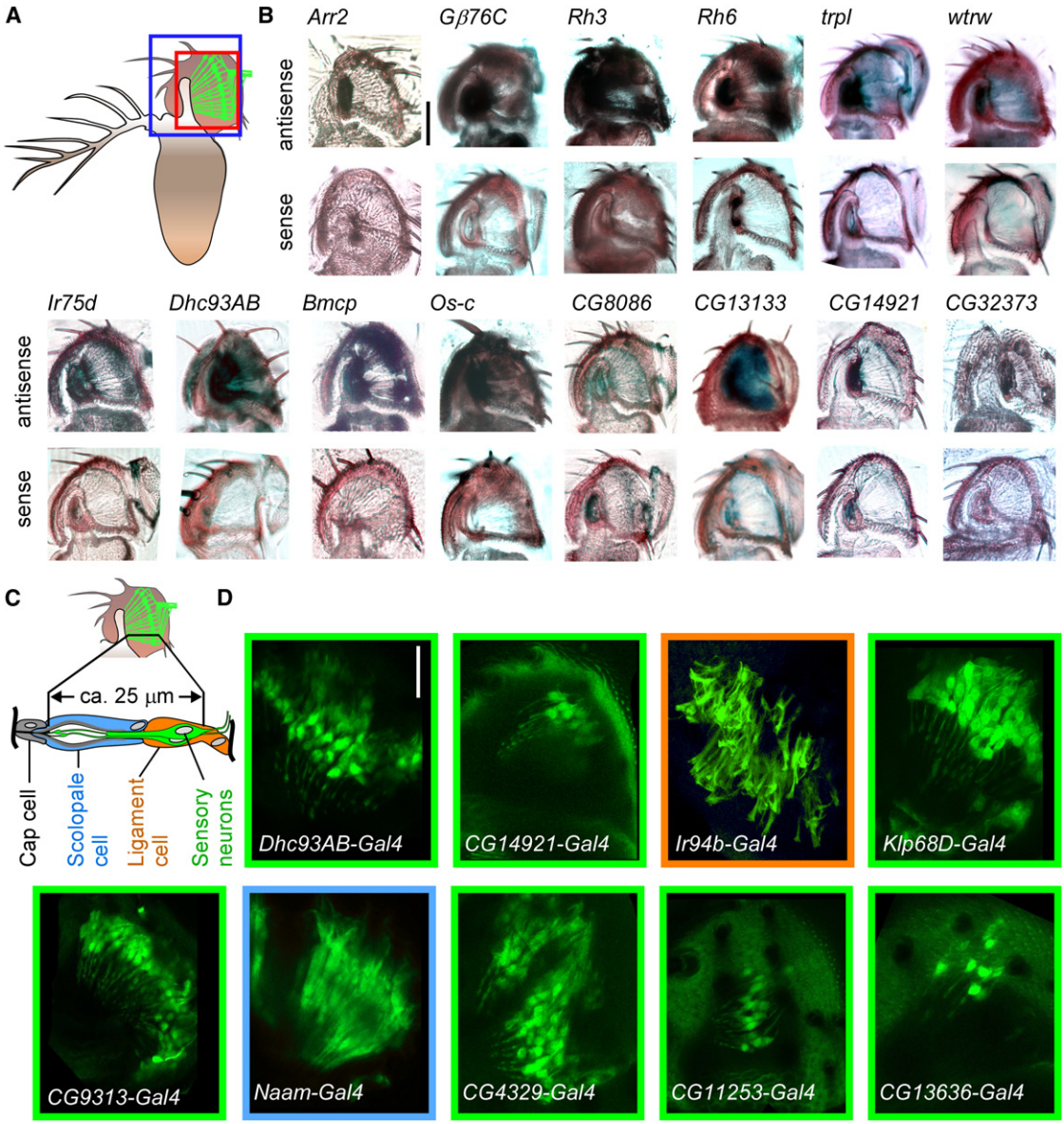

Figure 4. Gene Expression in the Auditory Organ

(A) Sketch of the antenna indicating the regions shown in (B) (blue box) and (D) (red box).

(B) Gene expression revealed by in situ hybridization with antisense probes and sense strand controls. Scale bar, 50 μm.

(C) Sketch of a chordotonal sensillum depicting its different cell types (bottom, modified from Sarpal et al. [2003]) and location of the sensilla in the second antennal segment (top, JO neurons depicted in green).

(D) Gene expression patterns in the second antennal segment revealed by driving UAS-2xEGFP via Gal4 promoter-fusion constructs (confocal sections). Frame colors indicate the identities of the labeled cells (color code as in C). Scale bar, 20 μm.

For a compilation of the expression data, please see Figure S3.

availability of point mutations or transposon insertions (Bellen et al., 2011). The alleles $wtrw^{E754K}$, in which a nucleic acid substitution (g2560a, isoform A) leads to the replacement of glutamic acid by lysine at position 754 (E754K), and $CG9313^{PADEF334P}$, in which a deletion of 12 nucleic acids (G1165–T1176) leads to the loss of four amino acids (P instead of PADEF), were identified by Tilling (Cooper et al., 2008). Transposons were crossed into w^{1118} or y^1w^{67c23} backgrounds and their effects on target gene transcription were assessed with qRT-PCR (Figures 5B and S1). To probe JO function, we exposed the flies to pure tones at the mechanical best frequency of their antennal receiver and recorded the resulting receiver displacement and compound action potentials (CAPs) from the antennal nerve (Effertz et al., 2011) (Figure 5A).

In wild-type (Canton S, Oregon R) and genetic background (w^{1118}, y^1w^{67c23}) strains, sound particle velocities above

~50 μm/s elicited CAPs that reached maximum amplitudes of ~50 μV. Antennal displacements consistently displayed a compressive nonlinearity that, arising from transducer-based mechanical amplification by auditory JO neurons (Nadrowski et al., 2008; Effertz et al., 2011), amplified receiver displacements ~10-fold when sound was faint (Figures 5B, 6A, and 6B).

Sound-evoked CAPs were eliminated by mutations in *CG9492* and *Dhc93AB*, which both encode dyneins, and in the *DYX1C1* homolog *CG14921* (Figures 5C and 6B). In the respective mutants, target gene transcripts were absent ($CG9492^{KG02504}$, $CG14921^{C247}$) or strongly reduced ($Dhc93AB^{MB05444}$), and mechanical amplification by JO neurons was virtually abolished with amplification gains of less than 1.5 (Figures 5C and 6B). Equally low amplification gains were caused by mutations in *Arr2*, *inaD*, *Rh5*, *Rh6*, *CG6053*, and *CG11253* (Figures 5D and 6B). In all these latter mutants, residual CAPs persisted, but the sound particle velocities required to elicit CAPs were significantly increased. Hence, mutations in 9 (21%) of the 42 genes severely impair JO function, abolishing mechanical amplification by JO neurons and strongly affecting their electrical response.

Mutations in 16 (38%) of the 42 genes moderately impaired JO function as witnessed by mechanical amplification gains between 1.5 and 5 (Figures 5E, 5F, and 6B). CAPs thresholds were significantly increased by mutations in *gl*, *rdgA*, *trpl*, *trp*, *wtrw*, *sei*, *Bmcp*, *CG9313*, *Dhc36c*, *CG4329*, and *CG13636* (Figures 5E and 6B), but not in *CG14636*, *Ir75a*, *Ank2*, *stops*, and *CG8086* (Figures 5F and 6B). In several of the mutants, CAP amplitudes were reduced (Figure 6B).

Excess mechanical amplification with gains greater than 15 characterized Cam^{5}/Cam^{n339} (Nelson et al., 1997) and bw^{1} mutants (Figures 5G and 6B), in which also CAP thresholds were slightly, though not significantly, decreased. Their ears were hypersensitive in that faint sounds induced larger antennal displacements than in control flies, and their antennae continuously oscillated spontaneously in the absence of sound (Figures 6C).

No auditory phenotypes were detected in $ninaC^{MB02664}$, $norpA^{7}$ (Harris and Stark, 1977), $gol^{MB03006}$, $Sulf1^{MB11661}$, and $CG8419^{MB06410}$ mutants, whose antennal mechanics and CAPs resembled those of controls (Figures S1A and 6B). This lack of auditory phenotypes is unlikely to reflect a low efficiency of the mutations: phototransduction is eliminated in $norpA^{7}$ mutants (Harris and Stark, 1977), and transcript levels are elevated in $gol^{MB03006}$ mutants, possibly reflecting compensatory expression, and strongly reduced in $ninaC^{MB02664}$, $Sulf1^{MB11661}$, and $CG8419^{MB06410}$ mutants (Figure S1A). Mutations in the remaining ten genes caused mild though significant alterations in mechanical amplification or electrical responsiveness (Figures S1B and 6B), but additional experiments are needed to confirm these subtle effects. Collectively, the above analysis documents that mutations in at least 27 (64%) of the 42 genes alter JO sound responses, doubling the number of auditory relevant *Drosophila* genes (Table S1).

Auditory Organ Function and Rhodopsins

Mutations in *Rh5* and *Rh6* strongly impair mechanical amplification by—and sound-evoked electrical responses of—JO neurons (Figures 5D and 6). To gain insights into the auditory roles of these Rhs, we performed several tests. First, we expressed a genomic *Rh6* rescue construct (Vasiliauskas et al., 2011) in the $Rh6^{1}$ mutant background and found that mechanical amplification and electrical responses are restored (Figure 7A). Second, in $Rh5^{2}$, $Rh6^{1}$ double mutants (Vasiliauskas et al., 2011), mechanical amplification was virtually abolished as in the single mutants; the sound required to evoke CAPs, however, had to be twice as loud as in the single mutants, documenting non-redundant mutant phenotypes for different *Rhs* (Figure 7B). Third, mechanical and electrical JO responses were also impaired in $santa\text{-}maria^{1}$ mutants, in which the rhodopsin-bound visual chromophore fails to form (Wang et al., 2007). When wild-type *santa-maria* was expressed in the JO neurons of the mutants, JO function was restored (Figure 7C). Fourth, wild-type flies reared at 24:0, 12:12, and 0:24 hr light:dark conditions all displayed normal JO sound responses (Figure 7D), and stimulating the flies with light did not evoke antennal nerve responses, indicating that JO function is independent of light. Fifth, transmission electron microscopy revealed normal JO anatomies in $Rh5^{2}$, $Rh6^{1}$ double mutants; mechanosensory relevant structures including the sensory cilia, their rootlets, and their dendritic caps all seemed normal (Figure 7E), and we did not detect ultrastructural defects. Sixth, antibodies against Rh5- and Rh6-labeled JO neurons in wild-type flies but not in $Rh5^{2}$, $Rh6^{1}$ double mutants (Figure 7F). Labeling was confined to the cytoplasm of the somata and to the cilia, where it partly superimposed with antihorseradish peroxidase (HRP) staining (Figures 7F and 7G). Anti-HRP recognizes sugar residues on glycoproteins that are transported into the cilia were they are secreted in two bands into the scolopale space (Figure 7E) (Ma and Jarman, 2011). These bands, which persisted in $Rh5^{2}$, $Rh6^{1}$ mutants, where recognized by anti-Rh5 (Figures 7F and 7G). The distal band may be important for partitioning the cilia (Cook et al., 2008), and beyond this band punctate anti-Rh5 (Figure 7G) and anti-Rh6 (Figure S2) staining was observed in the cilia, extending far into their mechanosensitive tips. Seventh, to test whether Rhs are required for mechanotransduction, we rapidly deflected the fly's receiver with force steps and monitored correlates of mechanotransducer gating in its mechanical response (Figure 7H). Wild-type receivers displayed the characteristic nonlinear gating compliance that associates with antennal nerve responses and arises from the direct gating of mechanotransduction channels (Albert et al., 2007; Nadrowski et al., 2008). This gating compliance was reduced in $Rh5^{2}$ and $Rh6^{1}$ mutants and virtually abolished in $Rh5^{2}$, $Rh6^{1}$ double mutants, which was also reflected by the response of the antennal nerve. Gating compliance and nerve response were both restored when the genomic *Rh6* rescue construct was expressed in the $Rh6^{1}$ mutant background, confirming that mechanotransducer gating in JO neurons requires Rhs. Apparently, Rhs facilitate transducer gating in a nonredundant and light-independent manner in the mechanosensory neurons of JO.

DISCUSSION

Mechano-, photo-, and chemoreceptors are developmentally specified by bHLH transcription factors across taxa (Fritzsch et al., 2007). Using the *Drosophila* JO as an example, we have

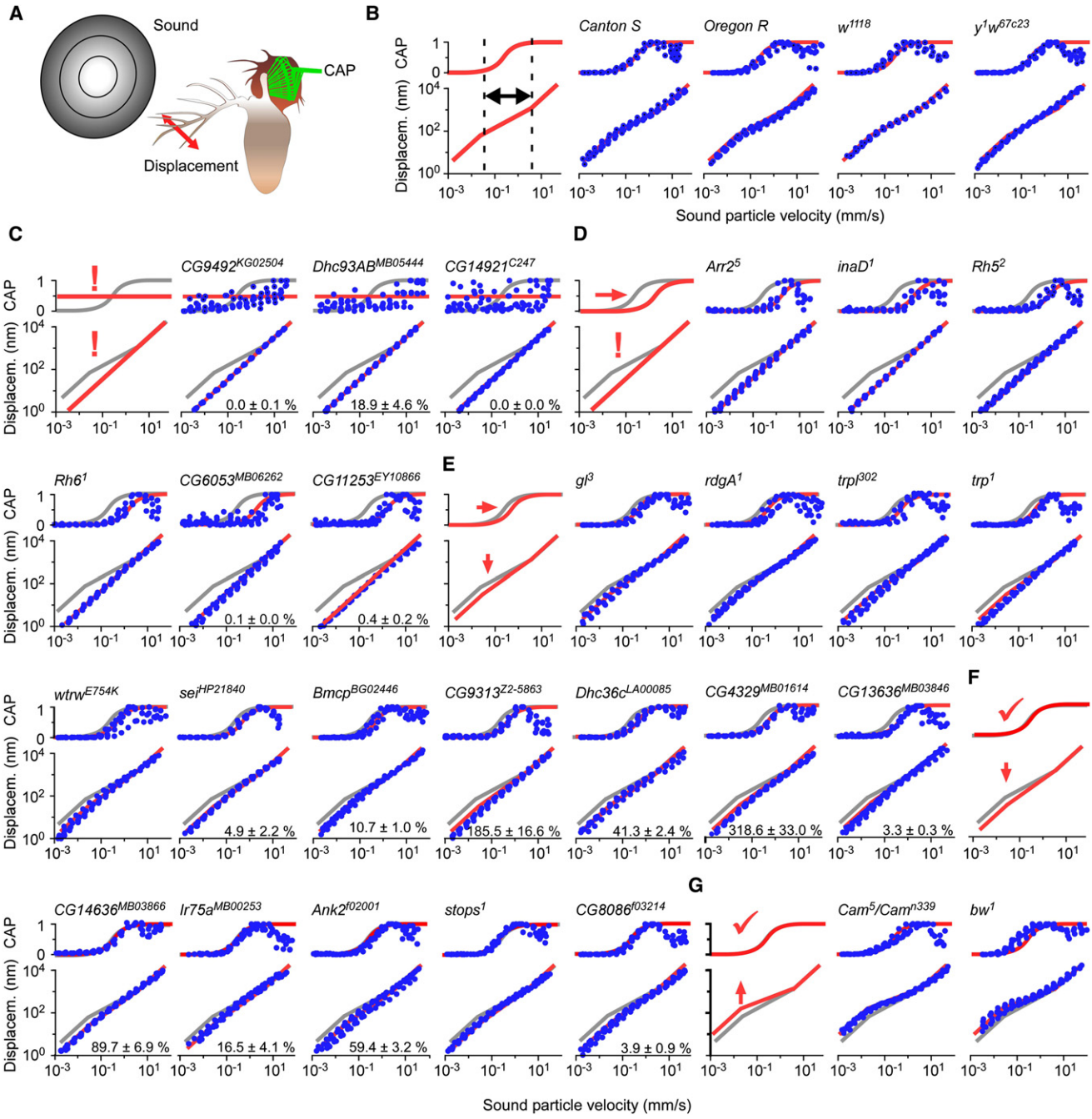

Figure 5. Auditory Organ Sound Responses in Controls and Mutants

(A) Experimental paradigm to assess auditory JO function. Flies were exposed to pure tones at the best frequency of their antennal receiver (Table S1) and the ensuing receiver displacement and CAP response were simultaneously assessed.

(B–G) Blue circles: relative CAP amplitudes (top) and receiver displacements (bottom) as functions of the sound particle velocity in controls (B) and mutants (C–G) (pooled data from five flies per strain). Relative CAP voltage (V) amplitudes are scaled from 0 to 1 and calculated as $(\boldsymbol{V} - \boldsymbol{V_{min}})/(\boldsymbol{V_{max}} - \boldsymbol{V_{min}})$. The first panels in (B)–(G) indicate the average slopes of the CAP (top) and displacement response (bottom) in the respective fly strains as red lines. In controls (B), displacement responses display a nonlinear regime at intermediate intensities (arrow) that is associated with the dynamic range of the CAPs (hatched lines) and arises from mechanical amplification by JO neurons. The lines from (B) are repeated as ghost traces in (C)–(G) to facilitate comparisons. Exclamation marks signal loss and arrows the direction and strength of significant deviations from controls (for significances, see Figure 6B). The absence of significant effects is indicated by ticks. Figures in the lower panels represent changes in transcript levels (%) with respect to w^{1118} controls (data are presented as mean ± SD, five technical replicates each).

(B) Controls. The receiver's displacement response displays a nonlinear regime at intermediate sound intensities (hatched lines and arrow) that aligns with the dynamic range of the CAPs and results from mechanical amplification by auditory JO neurons.

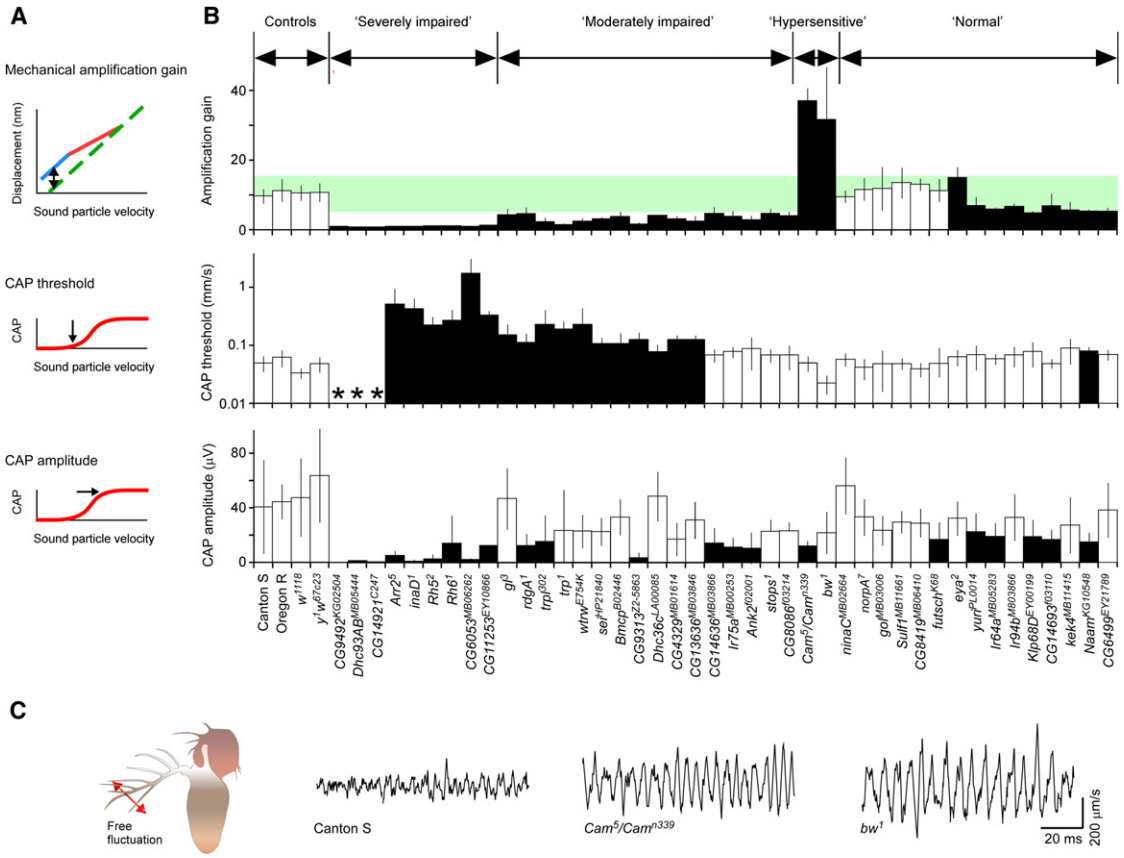

Figure 6. Auditory Response Characteristics

(A) Response parameters deduced from the data in Figures 5 and S1. For each individual fly, the gain of the mechanical amplification by JO neurons (top) was determined as the amplitude ratio (arrow) between the receiver's upper (green, hatched) and lower (blue) linear regimes. CAP thresholds (middle) were measured as the particle velocity corresponding to 10% of the maximum CAP amplitude as determined from Hill-fits, and the asymptotic value assumed by the fits was defined as the maximum voltage amplitude of the CAP response.

(B) Mechanical amplification gains (top), CAP thresholds (middle), and maximum CAP amplitudes (bottom) (data are presented as mean ± 1 SD, n = 5 flies per strain). Black bars indicate significant differences from controls ($p < 0.05$, two-tailed Mann-Whitney U tests against the pooled data from controls with Bonferroni correction for multiple comparisons). White bars indicate the absence of significant effects. Phenotypes are categorized based on their average mechanical sensitivity gain (<1.5: "severely impaired"; 1.5–5: "moderately impaired"; >15: "hypersensitive"). Average mechanical sensitivity gains between 5 and 15 (green area, upper panel) are considered "normal" even when significantly different from those of controls, providing a conservative judgment of auditory dysfunction.

(C) Time traces of the free mechanical fluctuations measured at the tip of the antennal arista (left) of a Canton S wild-type fly and Cam^5/Cam^{339n} and bw^1 mutants (right). In the mutants, the antennal receiver oscillates continuously in the absence of sound.

shown that null alleles of these transcription factors provide a background against which the genetic repertoire of the respective receptors can be defined. Ion channels and motors for fly hearing are identified that, judging from mutant phenotypes, contribute to auditory signal transduction. Some of the newly defined genes for hearing are also found in vertebrate cochleae, extending the genetic parallels between the ears of vertebrates and flies. In the fly, photo- and chemoreceptor proteins are expressed in the auditory organ and contribute to sound detection, adding new levels of complexity to auditory signal processing and shedding light on the evolution of *ato*-dependent receptor organs and sensory signaling cascades.

Auditory Stimulus Transduction, Axonemal Dyneins, and TRPs

Force-gated ion channels and adaptation motors are key constituents of auditory transduction modules (Gillespie and Müller, 2009), and their interplay provides mechanical amplification in the fly's ear (Nadrowski et al., 2008). The best candidate for the fly's auditory transducer is the NOMPC TRPN1 channel,

(C–G) Mutants. (C and D) JO function severely impaired: the displacement response is linearized, documenting the loss of mechanical amplification (average amplification gain <1.5, Figure 6B); CAPs are virtually lost (C) or only evoked by loud sounds (D). (E and F) JO function moderately impaired: nonlinear amplification is significantly reduced (average gain between 1.5 and 5) and CAPs are either significantly shifted to louder sounds (E) or not significantly altered (F). (G) JO hypersentitive: nonlinear amplification significantly increased (average gain >15) and CAP sensitivity unaltered. For statistics, see Figure 6.
For mutants with grossly normal JO function, please see Figure S1.

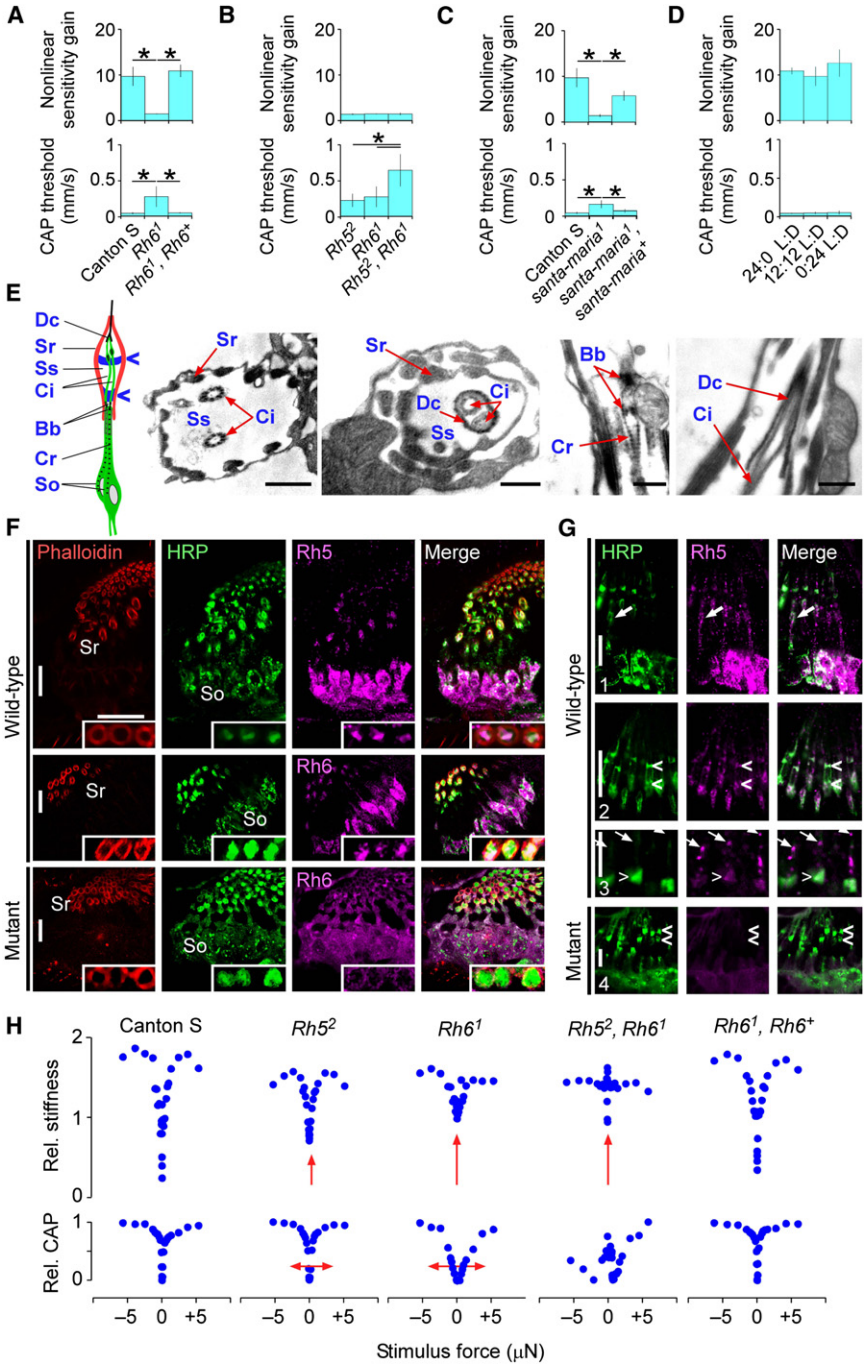

Figure 7. Rhodopsins in the Auditory Organ

(A) Genomic expression of wild-type *Rh6* (*Rh6*$^{+}$) rescues JO function in *Rh6*^{1} mutants, including the mechanical amplification gain (top) and CAP thresholds (bottom). Asterisks: $p < 0.05$ (two-tailed Mann-Whitney U tests).

(B) Nonlinear amplification is virtually abolished in single *Rh5*^{2} and *Rh6*^{1} and in *Rh5*^{2}, *Rh6*^{1} double mutants (top). In the latter flies, CAP thresholds are twice as high as in the single mutants (bottom).

(C) Impaired JO function in *santa-maria*^{1} mutants is rescued by expressing *UAS-santa-maria* in JO neurons using the Gal4 driver JO1 (Kamikouchi et al., 2009).

(D) JO sound responses are indistinguishable in Canton S wild-type flies grown at 24:0, 12:12, and 0:24 hr light:dark cycles.

(E) Sketch of a JO sensillum with two sensory neurons (left) and electron micrographs depicting sensory cilium structure in *Rh5*^{2}, *Rh6*^{1} double mutants (right). Dc, dendritic cap; Sr, scolopale rods; Ss, scolopale space; Ci, cilia; Bb, basal bodies; Cr, ciliary rootlets; So, somata. Blue arrowheads point to two the bands (depicted in blue) in the scolopale spaces that are recognized by anti-HRP. Scale bars, 0.5 μm.

(F) Fluorescence labeling of JO in wild-type flies and *Rh5*^{2}, *Rh6*^{1} double mutants. Phalloidin labels the scolopale rods (Sr) that surround the cilia and anti-HRP labels neuronal membranes. In the wild-type, anti-Rh5 and -Rh6 specifically label JO neuron somata and cilia whereas in the mutants only unspecific labeling is observed. Insets: cross-sections through the scolopales documenting colocalization of anti-HRP and anti-Rh5/anti-Rh6. In the mutants, unspecific anti-RH6 staining superimposes with phalloidin. Scale bars, 10 μm; insets 5 μm.

(G) Ciliary localization of Rhs. Row 1: anti-Rh5 staining of inner dendritic segments (arrows). Row 2, arrowheads: anti-Rh5 labeling of the two anti-HRP-positive bands in the scolopale space depicted in (E). Row 3: anti-Rh5 labeling extends from the distal bands (arrowhead) into the ciliary tips (arrows). Row 4: Persistence of anti-HRP-positive bands (arrowheads) in *Rh5*^{2}, *Rh6*^{1} double mutants. Scale bars, 10 μm (rows 1, 2, and 4) and 5 μm (row 3). For respective anti-Rh6 staining, please see Figure S2.

(H) Mechanical correlates of transducer gating. Relative dynamic stiffness of the antennal receiver as a function of the external stimulus force (top) and relative amplitudes of associated CAPs (bottom) in Canton S wild-type flies, *Rh5*^{2} and *Rh6*^{1} mutants, *Rh5*^{2}, *Rh6*^{1} double mutants, and *Rh6*^{1} mutants expressing wild-type *Rh6* (representative examples). Relative stiffness is measured as the ratio between the minimum dynamic stiffness of the receiver upon external forcing and the steady-state stiffness the receiver approaches when forcing is maintained. Red arrows highlight the reduced nonlinear gating compliance (top) of mutant receivers and the associated shift of the nerve response to larger forcing amplitudes (bottom). In the double mutants, gating compliance and CAPs are virtually abolished, and apparent residual signals largely represent noise.

See Figure S2.

whose *Caenorhabditis elegans* ortholog is a bona fide mechanotransduction channel (Kang et al., 2010) and which itself is essential for mechanical amplification (Göpfert et al., 2006; Effertz et al., 2011). Because JO neurons are ciliated and because their cilia seem to bear dynein arms, these cells were surmised to use axonemal dyneins as adaptation motors (Bechstedt and Howard, 2008). Our analysis shows that auditory phenotypes as reported for *nompC* nulls (Effertz et al., 2011)

also result from mutations in TRPC (TRP, TRPL) and TRPA (WTRW) channels, including the loss of mechanical amplification and sensitive nerve responses. Our analysis also shows that several axonemal dyneins are expressed in—and essential for the function of—JO neurons and that mutations in, e.g., the axonemal dynein gene *CG9313* lead to auditory defects as observed in *nompC* nulls (Effertz et al., 2011). Collectively, our results thus support axonemal dyneins as the presumptive adaptation motors in JO neurons and identify TRP channels (TRP, TRPL, WTRW) that, judging from their requirements for transducer-based amplification, contribute to transduction in the ear of the fly.

Genetic Parallels between Fly and Vertebrate Ears

Although JO neurons and hair cells are endowed with different sensory organelles and presumably use different channels and motors for auditory transduction and amplification, our analysis confirms and extends the genetic parallels between the ears of vertebrates and flies: 89 of the 274 JO genes have vertebrate homologs (Table S2), and several of these homologs occur in vertebrate ears: of the 27 auditory relevant JO genes, for example, calmodulin is found in hair cells where it regulates transducer adaptation (Walker and Hudspeth, 1996). This adaptation actuates active hair bundle motions, which promote—or contributes to—cochlear amplification in vertebrate ears (Hudspeth, 2008): low Ca^{2+} concentrations enhance amplification and lead to self-sustained hair bundle oscillations (Tinevez et al., 2007), consistent with the hyperamplification and ringing caused by mutations in *Drosophila Cam*. Hyperamplification also ensues from mutations in *bw*, which encodes an ATP-binding cassette (ABC) transporter. ABCs also occur in the mouse cochlea (e.g., Savary et al., 2007), but whether they contribute to cochlear function is unclear.

Also TRPC channels are found in vertebrate cochleae and outer hair cells reportedly express TRPC3 (Raybould et al., 2007). These cells also display a TRPC-like conductance that contributes to Ca^{2+} homeostasis and is activated via diacylglycerol (DAG) (Raybould et al., 2007). We found that mutations in the *Drosophila* DAG kinase gene *rdgA* cause auditory phenotypes as observed in TRPC channel mutants, and judged from the RIKEN full-length enriched cDNA library (Okazaki et al., 2002) a related DAG kinase, *DGKZ*, is expressed in the mouse inner ear (NCBI, library dbEST 9974). The same library also includes *ZSCAN22*, the homolog of *gl*, mutations in which impair JO function. *DYX1C1*, the homolog of the newly defined *Drosophila* deafness gene *CG14921*, in turn, is present in the Wackym-Soares normalized rat vestibular cDNA library (Roche et al., 2005; NCBI, library dbEST 16641), which also includes *Ank2* and the *Arr2* homolog *Arrb1*. *DYX1C1* is also expressed in the zebrafish otic vesicle (Thisse and Thisse, 2004), as is *zgc:63660*, the zebrafish homolog of the *Drosophila* deafness gene *CG11253*. Several of the fly genes for hearing thus seem present in vertebrate cochleae, putting forward new candidates for auditory relevant vertebrate genes.

Hearing with Chemo- and Photoreceptor Proteins and Sensory Organ Evolution

ato, apart from specifying chordotonal organs, directs the formation of *Drosophila* photoreceptors and chemosensory coeloconic sensilla (Jarman et al., 1994, 1995; Gupta and Rodrigues, 1997). All these receptors are thought to have evolved from an *ato*-dependent "protosensory" organ that presumably consisted of chordotonal sensilla because they are serially arranged along the body and distributed widely among arthropod groups (Niwa et al., 2004). Photoreceptors detect light with Rhs and coeloconic chemoreceptors detect volatile chemicals with IRs (Benton et al., 2009). The moderate auditory defects caused by mutations in IRs, along with the expression of *Ir94b* in JO supporting cells, suggest that these ion channels indirectly modulate JO neuron function, possibly by contributing to ion homeostasis in JO. Rhs, by contrast, are expressed in JO neurons and their disruption gravely impairs neuron function. Equally severe phenotypes result from the disruption of INAD, which holds together the fly's visual transduction complex (Chevesich et al., 1997; Scott and Zuker, 1998). Judging from our analysis, many components of this complex are expressed in JO, and Rhs occur in JO cilia and are required for proper mechanotransduction channel gating. Rhs, apart from sensing photons, have recently been put forward as thermosensors, documenting that they serve sensory functions other than detecting light (Shen et al., 2011). The involvement of IRs and Rhs in mechanosensory chordotonal organ function now suggests that these proteins already served roles in sensation before chemo- and photoreceptors have diversified. Given the presumed closeness of the "protosensory" organ and chordotonal organs (Niwa et al., 2004), we anticipate that dissecting IR and Rh functions in JO may help defining archetypical roles of these proteins, with the prospect of gaining a molecular understanding of how sensory modalities and signaling cascades evolved.

EXPERIMENTAL PROCEDURES

Flies were maintained according to German Federal regulations (license Gen.Az 501.40611/0166/501).

Gene Expression

The second antennal segments were isolated using microscissors, and their total RNA was amplified using a two-cycle protocol. cRNA was hybridized with Affymetrix Drosophila Genome 2.0 arrays. Gene Profile Analysis Suite (GEPAS, v. 4.0) was used for analysis (Herrero et al., 2003). qRT-PCRs were carried out with a MyiQ Single Color Real-Time PCR Detection System (BioRad). DIG-labeled (Roche DIG RNA Labeling Mix) riboprobes were generated by cloning gene specific cDNA fragments into the Invitrogen PCRII-TOPO Vector. Gene specific promoter-Gal4 transgenes were generated using the pPTGAL vector (Sharma et al., 2002). Confocal microscopy was carried out using a Leica TCS SP2 microscope.

Ultrastructure and Function

Electron microscopy was carried out on ultrathin sections using a Zeiss EM900 microscope. Antennal displacements were measured with a Polytec PSV-400 laser Doppler vibrometer, and resulting CAPs were recorded with a tungsten electrode inserted into the antenna's base. Antennae were actuated acoustically (Göpfert et al., 2006) and, to identify correlates of transducer gating, with electrostatic force (Albert et al., 2007).

ACCESSION NUMBERS

The complete microarray data is available from ArrayExpress (http://www.ebi.ac.uk/arrayexpress) under the submission name "Drosophila Johnston organ genes" (E-MEXP-3609).

SUPPLEMENTAL INFORMATION

Supplemental Information includes Extended Experimental Procedures, two figures, and four tables and can be found with this article online at http://dx.doi.org/10.1016/j.cell.2012.06.043.

ACKNOWLEDGEMENTS

We thank Claude Desplan, Roger Hardy, Charlotte Helfrich-Förster, Andrew Jarman, Bloomington Stock Centre, Exelixis Collection at Harvard Medical School, the Nippon Consortium, and Fly-Till for fly lines; BestGene, Inc. for fly injections; Steve Britt for antibodies; Thomas Effertz and Swantje Grätsch for help with physiology; and Matthias Schink and Torben Ruhwedel for technical support. This work was supported by the International Graduate School in Genetics and Functional Genomics (to P.R.S. and G.O.), the German National Academic Foundation (to D.P.), the Volkswagen Foundation (to B.N. and M.C.G.), the SFB 889 (A1 to M.C.G.) and a research grant from the DFG (Go1092/1-1, to M.C.G.).

Received: August 4, 2011
Revised: March 2, 2012
Accepted: June 20, 2012
Published: August 30, 2012

REFERENCES

Albert, J.T., Nadrowski, B., and Göpfert, M.C. (2007). Mechanical signatures of transducer gating in the *Drosophila* ear. Curr. Biol. *17*, 1000–1006.

Ashburner, M., Ball, C.A., Blake, J.A., Botstein, D., Butler, H., Cherry, J.M., Davis, A.P., Dolinski, K., Dwight, S.S., Eppig, J.T., et al.; The Gene Ontology Consortium. (2000). Gene ontology: tool for the unification of biology. Nat. Genet. *25*, 25–29.

Baker, D.A., Beckingham, K.M., and Armstrong, J.D. (2007). Functional dissection of the neural substrates for gravitaxic maze behavior in *Drosophila melanogaster*. J. Comp. Neurol. *501*, 756–764.

Bechstedt, S., and Howard, J. (2008). Hearing mechanics: a fly in your ear. Curr. Biol. *18*, R869–R870.

Bechstedt, S., Albert, J.T., Kreil, D.P., Müller-Reichert, T., Göpfert, M.C., and Howard, J. (2010). A doublecortin containing microtubule-associated protein is implicated in mechanotransduction in *Drosophila* sensory cilia. Nat. Commun. *1*, 11.

Bellen, H.J., Levis, R.W., He, Y., Carlson, J.W., Evans-Holm, M., Bae, E., Kim, J., Metaxakis, A., Savakis, C., Schulze, K.L., et al. (2011). The *Drosophila* gene disruption project: progress using transposons with distinctive site specificities. Genetics *188*, 731–743.

Benton, R., Vannice, K.S., Gomez-Diaz, C., and Vosshall, L.B. (2009). Variant ionotropic glutamate receptors as chemosensory receptors in *Drosophila*. Cell *136*, 149–162.

Bermingham, N.A., Hassan, B.A., Price, S.D., Vollrath, M.A., Ben-Arie, N., Eatock, R.A., Bellen, H.J., Lysakowski, A., and Zoghbi, H.Y. (1999). Math1: an essential gene for the generation of inner ear hair cells. Science *284*, 1837–1841.

Bloomquist, B.T., Shortridge, R.D., Schneuwly, S., Perdew, M., Montell, C., Steller, H., Rubin, G.M., and Pak, W.L. (1988). Isolation of a putative phospholipase C gene of *Drosophila, norpA*, and its role in phototransduction. Cell *54*, 723–733.

Cachero, S., Simpson, T.I., Zur Lage, P.I., Ma, L., Newton, F.G., Holohan, E.E., Armstrong, J.D., and Jarman, A.P. (2011). The gene regulatory cascade linking proneural specification with differentiation in *Drosophila* sensory neurons. PLoS Biol. *9*, e1000568.

Carbon, S., Ireland, A., Mungall, C.J., Shu, S., Marshall, B., Lewis, S., and Ami, G.O.AmiGO Hub; Web Presence Working Group. (2009). AmiGO: online access to ontology and annotation data. Bioinformatics *25*, 288–289.

Chevesich, J., Kreuz, A.J., and Montell, C. (1997). Requirement for the PDZ domain protein, INAD, for localization of the TRP store-operated channel to a signaling complex. Neuron *18*, 95–105.

Chien, S., Reiter, L.T., Bier, E., and Gribskov, M. (2002). Homophila: human disease gene cognates in *Drosophila*. Nucleic Acids Res. *30*, 149–151.

Chou, W.H., Huber, A., Bentrop, J., Schulz, S., Schwab, K., Chadwell, L.V., Paulsen, R., and Britt, S.G. (1999). Patterning of the R7 and R8 photoreceptor cells of *Drosophila*: evidence for induced and default cell-fate specification. Development *126*, 607–616.

Cook, B., Hardy, R.W., McConnaughey, W.B., and Zuker, C.S. (2008). Preserving cell shape under environmental stress. Nature *452*, 361–364.

Cooper, J.L., Till, B.J., and Henikoff, S. (2008). Fly-TILL: reverse genetics using a living point mutation resource. Fly (Austin) *2*, 300–302.

Dror, A.A., and Avraham, K.B. (2009). Hearing loss: mechanisms revealed by genetics and cell biology. Annu. Rev. Genet. *43*, 411–437.

Eberl, D.F., and Boekhoff-Falk, G. (2007). Development of Johnston's organ in *Drosophila*. Int. J. Dev. Biol. *51*, 679–687.

Eberl, D.F., Duyk, G.M., and Perrimon, N. (1997). A genetic screen for mutations that disrupt an auditory response in *Drosophila melanogaster*. Proc. Natl. Acad. Sci. USA *94*, 14837–14842.

Eberl, D.F., Hardy, R.W., and Kernan, M.J. (2000). Genetically similar transduction mechanisms for touch and hearing in Drosophila. J. Neurosci. *20*, 5981–5988.

Effertz, T., Wiek, R., and Göpfert, M.C. (2011). NompC TRP channel is essential for *Drosophila* sound receptor function. Curr. Biol. *21*, 592–597.

Fritzsch, B., Beisel, K.W., Pauley, S., and Soukup, G. (2007). Molecular evolution of the vertebrate mechanosensory cell and ear. Int. J. Dev. Biol. *51*, 663–678.

Gillespie, P.G., and Müller, U. (2009). Mechanotransduction by hair cells: models, molecules, and mechanisms. Cell *139*, 33–44.

Gong, Z., Son, W., Chung, Y.D., Kim, J., Shin, D.W., McClung, C.A., Lee, Y., Lee, H.W., Chang, D.J., Kaang, B.K., et al. (2004). Two interdependent TRPV channel subunits, inactive and Nanchung, mediate hearing in *Drosophila*. J. Neurosci. *24*, 9059–9066.

Göpfert, M.C., and Robert, D. (2001). Biomechanics. Turning the key on Drosophila audition. Nature *411*, 908.

Göpfert, M.C., Albert, J.T., Nadrowski, B., and Kamikouchi, A. (2006). Specification of auditory sensitivity by *Drosophila* TRP channels. Nat. Neurosci. *9*, 999–1000.

Gupta, B.P., and Rodrigues, V. (1997). *Atonal* is a proneural gene for a subset of olfactory sense organs in *Drosophila*. Genes Cells *2*, 225–233.

Haeberle, H., Fujiwara, M., Chuang, J., Medina, M.M., Panditrao, M.V., Bechstedt, S., Howard, J., and Lumpkin, E.A. (2004). Molecular profiling reveals synaptic release machinery in Merkel cells. Proc. Natl. Acad. Sci. USA *101*, 14503–14508.

Hardie, R.C., and Minke, B. (1992). The *trp* gene is essential for a light-activated Ca^{2+} channel in *Drosophila* photoreceptors. Neuron *8*, 643–651.

Harris, W.A., and Stark, W.S. (1977). Hereditary retinal degeneration in Drosophila melanogaster. A mutant defect associated with the phototransduction process. J. Gen. Physiol. *69*, 261–291.

Herrero, J., Al-Shahrour, F., Díaz-Uriarte, R., Mateos, A., Vaquerizas, J.M., Santoyo, J., and Dopazo, J. (2003). GEPAS: A web-based resource for microarray gene expression data analysis. Nucleic Acids Res. *31*, 3461–3467.

Hildebrand, M.S., Newton, S.S., Gubbels, S.P., Sheffield, A.M., Kochhar, A., de Silva, M.G., Dahl, H.H., Rose, S.D., Behlke, M.A., and Smith, R.J. (2008). Advances in molecular and cellular therapies for hearing loss. Mol. Ther. *16*, 224–236.

Hudspeth, A.J. (2008). Making an effort to listen: mechanical amplification in the ear. Neuron *59*, 530–545.

Jarman, A.P., Grau, Y., Jan, L.Y., and Jan, Y.N. (1993). *atonal* is a proneural gene that directs chordotonal organ formation in the *Drosophila* peripheral nervous system. Cell *73*, 1307–1321.

Jarman, A.P., Grell, E.H., Ackerman, L., Jan, L.Y., and Jan, Y.N. (1994). *Atonal* is the proneural gene for *Drosophila* photoreceptors. Nature *369*, 398–400.

Jarman, A.P., Sun, Y., Jan, L.Y., and Jan, Y.N. (1995). Role of the proneural gene, *atonal*, in formation of *Drosophila* chordotonal organs and photoreceptors. Development *121*, 2019–2030.

Kamikouchi, A., Inagaki, H.K., Effertz, T., Hendrich, O., Fiala, A., Göpfert, M.C., and Ito, K. (2009). The neural basis of *Drosophila* gravity-sensing and hearing. Nature *458*, 165–171.

Kang, L., Gao, J., Schafer, W.R., Xie, Z., and Xu, X.Z. (2010). *C. elegans* TRP family protein TRP-4 is a pore-forming subunit of a native mechanotransduction channel. Neuron *67*, 381–391.

Kapushesky, M., Kemmeren, P., Culhane, A.C., Durinck, S., Ihmels, J., Körner, C., Kull, M., Torrente, A., Sarkans, U., Vilo, J., and Brazma, A. (2004). Expression Profiler: next generation–an online platform for analysis of microarray data. Nucleic Acids Res. *32*, W465–470.

Kavlie, R.G., Kernan, M.J., and Eberl, D.F. (2010). Hearing in *Drosophila* requires TilB, a conserved protein associated with ciliary motility. Genetics *185*, 177–188.

Kernan, M., Cowan, D., and Zuker, C. (1994). Genetic dissection of mechanosensory transduction: mechanoreception-defective mutations of *Drosophila*. Neuron *12*, 1195–1206.

Kim, J., Chung, Y.D., Park, D.Y., Choi, S., Shin, D.W., Soh, H., Lee, H.W., Son, W., Yim, J., Park, C.S., et al. (2003). A TRPV family ion channel required for hearing in *Drosophila*. Nature *424*, 81–84.

Laurençon, A., Dubruille, R., Efimenko, E., Grenier, G., Bissett, R., Cortier, E., Rolland, V., Swoboda, P., and Durand, B. (2007). Identification of novel regulatory factor X (RFX) target genes by comparative genomics in *Drosophila* species. Genome Biol. *8*, R195.

Liedtke, W., Choe, Y., Martí-Renom, M.A., Bell, A.M., Denis, C.S., Sali, A., Hudspeth, A.J., Friedman, J.M., and Heller, S. (2000). Vanilloid receptor-related osmotically activated channel (VR-OAC), a candidate vertebrate osmoreceptor. Cell *103*, 525–535.

Liu, L., Li, Y., Wang, R., Yin, C., Dong, Q., Hing, H., Kim, C., and Welsh, M.J. (2007). *Drosophila* hygrosensation requires the TRP channels water witch and nanchung. Nature *450*, 294–298.

Livak, K.J., and Schmittgen, T.D. (2001). Analysis of relative gene expression data using real-time quantitative PCR and the $2^{(-\Delta\ \Delta\ C(T))}$ Method. Methods *25*, 402–408.

Lu, Q., Senthilan, P.R., Effertz, T., Nadrowski, B., and Göpfert, M.C. (2009). Using *Drosophila* for studying fundamental processes in hearing. Integr. Comp. Biol. *49*, 674–680.

Ma, L., and Jarman, A.P. (2011). Dilatory is a *Drosophila* protein related to AZI1 (CEP131) that is located at the ciliary base and required for cilium formation. J. Cell Sci. *124*, 2622–2630.

McKenna, M.P., Hekmat-Scafe, D.S., Gaines, P., and Carlson, J.R. (1994). Putative *Drosophila* pheromone-binding proteins expressed in a subregion of the olfactory system. J. Biol. Chem. *269*, 16340–16347.

McDermott, B.M., Jr., Baucom, J.M., and Hudspeth, A.J. (2007). Analysis and functional evaluation of the hair-cell transcriptome. Proc. Natl. Acad. Sci. USA *104*, 11820–11825.

Miron, M., Woody, O.Z., Marcil, A., Murie, C., Sladek, R., and Nadon, R.A. (2006). A methodology for global validation of microarray experiments. BMC Bioinformatics *7*, 333.

Montell, C., Jones, K., Hafen, E., and Rubin, G. (1985). Rescue of the *Drosophila* phototransduction mutation *trp* by germline transformation. Science *230*, 1040–1043.

Nadrowski, B., Albert, J.T., and Göpfert, M.C. (2008). Transducer-based force generation explains active process in *Drosophila* hearing. Curr. Biol. *18*, 1365–1372.

Nelson, H.B., Heiman, R.G., Bolduc, C., Kovalick, G.E., Whitley, P., Stern, M., and Beckingham, K. (1997). Calmodulin point mutations affect *Drosophila* development and behavior. Genetics *147*, 1783–1798.

Niemeyer, B.A., Suzuki, E., Scott, K., Jalink, K., and Zuker, C.S. (1996). The *Drosophila* light-activated conductance is composed of the two channels TRP and TRPL. Cell *85*, 651–659.

Niwa, N., Hiromi, Y., and Okabe, M. (2004). A conserved developmental program for sensory organ formation in Drosophila melanogaster. Nat. Genet. *36*, 293–297.

Okazaki, Y., Furuno, M., Kasukawa, T., Adachi, J., Bono, H., Kondo, S., Nikaido, I., Osato, N., Saito, R., Suzuki, H., et al.; FANTOM Consortium; RIKEN Genome Exploration Research Group Phase I & II Team. (2002). Analysis of the mouse transcriptome based on functional annotation of 60,770 full-length cDNAs. Nature *420*, 563–573.

Petit, C. (2006). From deafness genes to hearing mechanisms: harmony and counterpoint. Trends Mol. Med. *12*, 57–64.

Raybould, N.P., Jagger, D.J., Kanjhan, R., Greenwood, D., Laslo, P., Hoya, N., Soeller, C., Cannell, M.B., and Housley, G.D. (2007). TRPC-like conductance mediates restoration of intracellular Ca^{2+} in cochlear outer hair cells in the guinea pig and rat. J. Physiol. *579*, 101–113.

Roche, J.P., Wackym, P.A., Cioffi, J.A., Kwitek, A.E., Erbe, C.B., and Popper, P. (2005). In silico analysis of 2085 clones from a normalized rat vestibular periphery 3′ cDNA library. Audiol. Neurootol. *10*, 310–322.

Rosenzweig, M., Kang, K., and Garrity, P.A. (2008). Distinct TRP channels are required for warm and cool avoidance in *Drosophila melanogaster*. Proc. Natl. Acad. Sci. USA *105*, 14668–14673.

Sarpal, R., Todi, S.V., Sivan-Loukianova, E., Shirolikar, S., Subramanian, N., Raff, E.C., Erickson, J.W., Ray, K., and Eberl, D.F. (2003). *Drosophila* KAP interacts with the kinesin II motor subunit KLP64D to assemble chordotonal sensory cilia, but not sperm tails. Curr. Biol. *13*, 1687–1696.

Savary, E., Hugnot, J.P., Chassigneux, Y., Travo, C., Duperray, C., Van De Water, T., and Zine, A. (2007). Distinct population of hair cell progenitors can be isolated from the postnatal mouse cochlea using side population analysis. Stem Cells *25*, 332–339.

Schaeffer, E., Smith, D., Mardon, G., Quinn, W., and Zuker, C.S. (1989). Isolation and characterization of two new *drosophila* protein kinase C genes, including one specifically expressed in photoreceptor cells. Cell *57*, 403–412.

Schulz, S., Huber, A., Schwab, K., and Paulsen, R. (1999). A novel Ggamma isolated from Drosophila constitutes a visual G protein gamma subunit of the fly compound eye. J. Biol. Chem. *274*, 37605–37610.

Scott, K., and Zuker, C.S. (1998). Assembly of the *Drosophila* phototransduction cascade into a signalling complex shapes elementary responses. Nature *395*, 805–808.

Sharma, Y., Cheung, U., Larsen, E.W., and Eberl, D.F. (2002). PPTGAL, a convenient Gal4 P-element vector for testing expression of enhancer fragments in *drosophila*. Genesis *34*, 115–118.

Shen, W.L., Kwon, Y., Adegbola, A.A., Luo, J., Chess, A., and Montell, C. (2011). Function of rhodopsin in temperature discrimination in *Drosophila*. Science *331*, 1333–1336.

Shieh, B.H., and Niemeyer, B. (1995). A novel protein encoded by the *InaD* gene regulates recovery of visual transduction in *Drosophila*. Neuron *14*, 201–210.

Sidi, S., Friedrich, R.W., and Nicolson, T. (2003). NompC TRP channel required for vertebrate sensory hair cell mechanotransduction. Science *301*, 96–99.

Thisse, B., and Thisse, C. (2004). Fast release clones: a high throughput expression analysis. ZFIN direct data submission (http://zfin.org).

Tinevez, J.-Y., Jülicher, F., and Martin, P. (2007). Unifying the various incarnations of active hair-bundle motility by the vertebrate hair cell. Biophys. J. *93*, 4053–4067.

Todi, S.V., Franke, J.D., Kiehart, D.P., and Eberl, D.F. (2005). Myosin VIIA defects, which underlie the Usher 1B syndrome in humans, lead to deafness in *Drosophila*. Curr. Biol. *15*, 862–868.

Vasiliauskas, D., Mazzoni, E.O., Sprecher, S.G., Brodetskiy, K., Johnston, R.J., Jr., Lidder, P., Vogt, N., Celik, A., and Desplan, C. (2011). Feedback from

rhodopsin controls rhodopsin exclusion in *Drosophila* photoreceptors. Nature *479*, 108–112.

Walker, R.G., and Hudspeth, A.J. (1996). Calmodulin controls adaptation of mechanoelectrical transduction by hair cells of the bullfrog's sacculus. Proc. Natl. Acad. Sci. USA *93*, 2203–2207.

Walker, R.G., Willingham, A.T., and Zuker, C.S. (2000). A *Drosophila* mechanosensory transduction channel. Science *287*, 2229–2234.

Wang, T., Jiao, Y., and Montell, C. (2007). Dissection of the pathway required for generation of vitamin A and for *Drosophila* phototransduction. J. Cell Biol. *177*, 305–316.

Weber, T., Göpfert, M.C., Winter, H., Zimmermann, U., Kohler, H., Meier, A., Hendrich, O., Rohbock, K., Robert, D., and Knipper, M. (2003). Expression of prestin-homologous solute carrier (SLC26) in auditory organs of nonmammalian vertebrates and insects. Proc. Natl. Acad. Sci. USA *100*, 7690–7695.

Weil, D., Blanchard, S., Kaplan, J., Guilford, P., Gibson, F., Walsh, J., Mburu, P., Varela, A., Levilliers, J., Weston, M.D., et al. (1995). Defective myosin VIIA gene responsible for Usher syndrome type 1B. Nature *374*, 60–61.

Yamada, T., Takeuchi, Y., Komori, N., Kobayashi, H., Sakai, Y., Hotta, Y., and Matsumoto, H. (1990). A 49-kilodalton phosphoprotein in the *Drosophila* photoreceptor is an arrestin homolog. Science *248*, 483–486.

Yarfitz, S., Niemi, G.A., McConnell, J.L., Fitch, C.L., and Hurley, J.B. (1991). A G beta protein in the Drosophila compound eye is different from that in the brain. Neuron *7*, 429–438.

Yorozu, S., Wong, A., Fischer, B.J., Dankert, H., Kernan, M.J., Kamikouchi, A., Ito, K., and Anderson, D.J. (2009). Distinct sensory representations of wind and near-field sound in the *Drosophila* brain. Nature *458*, 201–205.

Zheng, J., Shen, W., He, D.Z.Z., Long, K.B., Madison, L.D., and Dallos, P. (2000). Prestin is the motor protein of cochlear outer hair cells. Nature *405*, 149–155.